

Hyperon Puzzle: Hints from Quantum Monte Carlo Calculations

Diego Lonardonì,¹ Alessandro Lovato,¹ Stefano Gandolfi,² and Francesco Pederiva^{3,4}
¹*Physics Division, Argonne National Laboratory, Lemont, Illinois 60439, USA*
²*Theoretical Division, Los Alamos National Laboratory, Los Alamos, New Mexico 87545, USA*
³*Physics Department, University of Trento, via Sommarive, 14 I-38123 Trento, Italy*
⁴*INFN-TIFPA, Trento Institute for Fundamental Physics and Applications, I-38123 Trento, Italy*
 (Received 24 July 2014; published 6 March 2015)

The onset of hyperons in the core of neutron stars and the consequent softening of the equation of state have been questioned for a long time. Controversial theoretical predictions and recent astrophysical observations of neutron stars are the grounds for the so-called *hyperon puzzle*. We calculate the equation of state and the neutron star mass-radius relation of an infinite systems of neutrons and Λ particles by using the auxiliary field diffusion Monte Carlo algorithm. We find that the three-body hyperon-nucleon interaction plays a fundamental role in the softening of the equation of state and for the consequent reduction of the predicted maximum mass. We have considered two different models of three-body force that successfully describe the binding energy of medium mass hypernuclei. Our results indicate that they give dramatically different results on the maximum mass of neutron stars, not necessarily incompatible with the recent observation of very massive neutron stars. We conclude that stronger constraints on the hyperon-neutron force are necessary in order to properly assess the role of hyperons in neutron stars.

DOI: 10.1103/PhysRevLett.114.092301

PACS numbers: 26.60.Kp, 13.75.Ev, 21.65.Cd

In their pioneering work, Ambartsumyan and Saakyan reported the first theoretical indication for the appearance of hyperons in the core of a neutron star (NS) [1]. In terrestrial conditions hyperons are unstable and decay into nucleons through weak interactions. On the contrary, in the degenerate dense matter forming the inner core of a NS, Pauli blocking prevents hyperons from decaying by limiting the phase space available to nucleons. When the nucleon chemical potential is large enough, the creation of hyperons from nucleons is energetically favorable. This leads to a reduction of the Fermi pressure exerted by the baryons and, as a consequence, to a softening of the equation of state (EOS) and to a reduction of the predicted maximum mass.

Currently there is no general agreement (even qualitative) among the predicted results for the EOS and the maximum mass of a NS including hyperons. Some of the standard nuclear physics many-body approaches, such as Hartree-Fock [2,3], Brueckner-Hartree-Fock [4,5] or the extended Quark Mean Field model [6], predict the appearance of hyperons at a density of $(2-3)\rho_0$, $\rho_0 = 0.16 \text{ fm}^{-3}$, and a strong softening of the EOS, implying a sizable reduction of the maximum mass. On the other hand, other approaches like relativistic Hartree-Fock [7,8], relativistic mean field models [9–14] or quantum hadrodynamics [15] indicate much weaker effects as a consequence of the presence of strange baryons in the core of a NS. It should be noted that several of the parameters entering these models cannot be fully constrained by the available experimental data.

The value of about $1.4M_\odot$ for the maximum mass of a NS, inferred from neutron star mass determinations [16], was generally considered the canonical limit. The measurements of the large mass values of the millisecond pulsars PSR J1903 + 0327 ($1.67(2)M_\odot$) [17] and in particular PSR J1614-2230 ($1.97(4)M_\odot$) [18] and PSR J0348 + 0432 ($2.01(4)M_\odot$) [19] suggest a stiff EOS. Other NS observations of masses and radii seem to disfavor a very soft EOS of neutron star matter [20–23]. This seems to contradict the appearance of strange baryons in high-density matter, at least according to nonrelativistic many-body approaches.

In the last few years new models compatible with the recent observations have been proposed. Current astrophysical and laboratory data have been used as constraints for a hypernuclear density functional theory [24]. The phase transition to confined or deconfined quark matter has been investigated by several authors [25–28]. More exotic EOSs, including hyperons and the antikaon condensate, have been also formulated, as reported for instance in Ref. [29]. Evidence for the need of a universal many-baryons repulsion has been suggested [30,31] and employed in nuclear and hypernuclear matter calculations [32,33]. However, many inconsistencies still remain. The solution to this problem, known as the *hyperon puzzle*, is still far from understood.

In this Letter we present the first quantum Monte Carlo analysis of infinite matter composed of neutrons and Λ particles. In Refs. [34,35] it has been shown that within a phenomenological approach similar to the construction of the Argonne-Illinois nucleon-nucleon interaction, a repulsive three-body hyperon-nucleon force is needed to

reproduce the ground state properties of medium-light Λ hypernuclei. The repulsive three-body force dramatically affects the EOS, and the inclusion of Λ particles in neutron matter does not necessarily produce a NS with maximum mass that is incompatible with recent observations. In our calculations, the effect of the presence of hyperons other than the Λ has not been investigated. Their interaction with the neutrons is even less constrained than the Λ -nucleon one. Moreover, as our results clearly show that different three-body forces give a very different EOS, we stress the fact that more constraints on the hyperon-neutron force are needed before drawing any conclusion on the role played by hyperons in neutron stars.

Within nonrelativistic many-body approaches, hyperneutron matter (HNM) can be described in terms of pointlike neutrons and lambdas, with masses m_n and m_Λ , respectively, whose dynamics are dictated by the Hamiltonian

$$H = \sum_i \frac{p_i^2}{2m_n} + \sum_\lambda \frac{p_\lambda^2}{2m_\Lambda} + \sum_{i<j} v_{ij} + \sum_{i<j<k} v_{ijk} + \sum_{\lambda,i} v_{\lambda i} + \sum_{\lambda,i<j} v_{\lambda ij}, \quad (1)$$

where we use i and j to indicate nucleons, and λ to indicate Λ particles. In our calculation, the two-nucleon interaction v_{ij} is the Argonne V8' (AV8') potential [36], that is a re-projection of the more sophisticated Argonne AV18 [37], but is simpler to be included in our calculation. It gives the largest contributions to the nucleon-nucleon interaction, moderately more attractive than AV18 in light nuclei [38] but very similar to AV18 in neutron drops [39,40]. The v_{ijk} is the Urbana IX (UIX) three-body potential, that was originally fitted to the triton and α particle binding energies and to reproduce the empirical saturation density of nuclear matter when used with AV18 [41]. The AV8'+UIX Hamiltonian has been extensively used to investigate properties of neutron matter and neutron stars (see for instance Refs. [20,42,43]).

For the hyperon sector, we adopted the phenomenological hyperon-nucleon potential that was first introduced by Bodmer, Usmani, and Carlson in a similar fashion to the Argonne and Urbana interactions [44]. It has been employed in several calculations of light hypernuclei [45–51] and, more recently, to study the structure of light and medium mass Λ hypernuclei [34,35]. The two-body ΛN interaction, $v_{\lambda i}$, includes central and spin-spin components and it has been fitted on the available hyperon-nucleon scattering data. A charge symmetry breaking term was introduced in order to describe the energy splitting in the mirror Λ hypernuclei for $A = 4$ [34,47]. The three-body ΛNN force, $v_{\lambda ij}$, includes contributions coming from P - and S -wave 2π exchange plus a phenomenological repulsive term. In this work we have considered two different parametrizations of the ΛNN force.

The authors of Ref. [49] reported a parametrization, hereafter referred to as parametrization (I), that simultaneously reproduces the hyperon separation energy of ${}^5_\Lambda\text{He}$ and ${}^{17}_\Lambda\text{O}$ obtained using variational Monte Carlo techniques. In Ref. [34], a diffusion Monte Carlo study of a wide range of Λ hypernuclei up to $A = 91$ has been performed. Within that framework, additional repulsion has been included in order to satisfactorily reproduce the experimental hyperon separation energies. We refer to this model of ΛNN interaction as parametrization (II).

No $\Lambda\Lambda$ potential has been included in the calculation. Its determination is limited by the fact that $\Lambda\Lambda$ scattering data are not available and experimental information about double Λ hypernuclei is scarce. The most advanced theoretical works discussing $\Lambda\Lambda$ force [52,53], show that it is indeed rather weak. Hence, its effect is believed to be negligible for the purpose of this work. Self-bound multi-strange systems have been investigated within the relativistic mean field framework [54–56]. However, hyperons other than Λ have not been taken into account in the present study due to the lack of potential models suitable for quantum Monte Carlo calculations.

To compute the EOS of HNM we employed the auxiliary field diffusion Monte Carlo (AFDMC) algorithm [57], which has been successfully applied to investigate properties of pure neutron matter (PNM) [40,43,58–60]. Within AFDMC calculations, the solution of the many-body Schrödinger equation is obtained by enhancing the ground-state component of the starting trial wave function using the imaginary-time projection technique. In order to efficiently deal with spin-isospin dependent Hamiltonians, the Hubbard-Stratonovich transformation is applied to the imaginary time propagator. This procedure reduces the dependence of spin-isospin operators from quadratic to linear, lowering the computational cost of the calculation from exponential to polynomial in the number of particles allowing for the study of many-nucleon systems.

The extension of AFDMC calculations to finite hypernuclear systems has been discussed in detail in Ref. [34]. Following the same line, we have further developed the algorithm to deal with infinite hyperneutron matter. The PNM trial wave function has been extended by including a Slater determinant of plane waves and two-component spinors for the Λ particles. The propagation in imaginary time now involves the sampling of the coordinates and the rotation of the spinors induced by the Hubbard-Stratonovich transformation for both neutrons and hyperons. The Fermion sign problem is controlled via the constrained-path prescription [59] with a straightforward extension to the enlarged hyperon-nucleon space. The expectation values are evaluated as in the standard AFDMC method, as reported in Ref. [34].

Hyperneutron matter is composed of neutrons and a fraction $x = \rho_\Lambda/\rho$ of Λ hyperons, where $\rho = \rho_n + \rho_\Lambda$ is the total baryon density of the system, $\rho_n = (1-x)\rho$ and

$\rho_\Lambda = x\rho$ are the neutron and hyperon densities, respectively. The energy per particle can be written as

$$E_{\text{HNM}}(\rho, x) = [E_{\text{PNM}}((1-x)\rho) + m_n](1-x) + [E_{\text{P}\Lambda\text{M}}(x\rho) + m_\Lambda]x + f(\rho, x). \quad (2)$$

To deal with the mass difference $\Delta m \simeq 176$ MeV between neutrons and lambdas the rest energy is explicitly taken into account. The energy per particle of PNM E_{PNM} has been calculated using the AFDMC method [42,43] and it reads

$$E_{\text{PNM}}(\rho_n) = a \left(\frac{\rho_n}{\rho_0} \right)^\alpha + b \left(\frac{\rho_n}{\rho_0} \right)^\beta, \quad (3)$$

where the parameters a , α , b , and β are reported in Table I.

We parametrized the energy of pure lambda matter $E_{\text{P}\Lambda\text{M}}$ with the Fermi gas energy of noninteracting Λ particles. Such a formulation is suggested by the fact that in the Hamiltonian of Eq. (1) there is no $\Lambda\Lambda$ potential. The reason for parametrizing the energy per particle of hyperneutron matter as in Eq. (2) lies in the fact that, within AFDMC calculations, $E_{\text{HNM}}(\rho, x)$ can be easily evaluated only for a discrete set of x values. They correspond to a different number of neutrons ($N_n = 66, 54, 38$) and hyperons ($N_\Lambda = 1, 2, 14$) in the simulation box giving momentum closed shells. Hence, the function $f(\rho, x)$ provides an analytical parametrization for the difference between Monte Carlo energies of hyperneutron matter and pure neutron matter in the (ρ, x) domain that we have considered. Corrections for the finite-size effects due to the interaction are included as described in Ref. [60] for both nucleon-nucleon and hyperon-nucleon forces. Finite-size effects on the neutron kinetic energy arising when using different number of neutrons have been corrected adopting the same technique described in Ref. [61]. Possible additional finite-size effects for the hypernuclear systems have been reduced by considering energy differences between HNM and PNM calculated in the same simulation box, and by correcting for the (small) change of neutron density.

As can be inferred by Eq. (2), both hyperon-nucleon potential and correlations contribute to $f(\rho, x)$, whose dependence on ρ and x can be conveniently exploited within a cluster expansion scheme. Our parametrization is

$$f(\rho, x) = c_1 \frac{x(1-x)\rho}{\rho_0} + c_2 \frac{x(1-x)^2\rho^2}{\rho_0^2}. \quad (4)$$

Because the $\Lambda\Lambda$ potential has not been included in the model, we have only considered clusters with at most one

TABLE I. Fitting parameters for the neutron matter EOS of Eq. (3) [42].

a [MeV]	α	b [MeV]	β
13.4(1)	0.514(3)	5.62(5)	2.436(5)

Λ . We checked that contributions coming from clusters of two or more hyperons and three or more neutrons give negligible contributions in the fitting procedure. We have also tried other functional forms for $f(x, \rho)$, including polytropes inspired by those of Ref. [20]. Moreover, we have fitted the Monte Carlo results using different x data sets. The final results weakly depend on the choice of parametrization and on the fit range, in particular for the hyperon threshold density. The resulting EOSs and mass-radius relations are represented by the shaded bands in Fig. 1 and Fig. 2. The parameters c_1 and c_2 corresponding to the centroids of the figures are listed in Table II.

Once $f(\rho, x)$ has been fitted, the chemical potentials for neutrons and lambdas are evaluated via

$$\mu_n(\rho, x) = \frac{\partial \mathcal{E}_{\text{HNM}}}{\partial \rho_n}, \quad \mu_\Lambda(\rho, x) = \frac{\partial \mathcal{E}_{\text{HNM}}}{\partial \rho_\Lambda}, \quad (5)$$

where $\mathcal{E}_{\text{HNM}} = \rho E_{\text{HNM}}$ is the energy density. The hyperon fraction as a function of the baryon density, $x(\rho)$, is obtained by imposing the condition $\mu_\Lambda = \mu_n$. The Λ threshold density ρ_Λ^{th} is determined where $x(\rho)$ starts being different from zero.

In Fig. 1 the EOS for PNM (green solid curve) and HNM using the two-body ΛN interaction alone (red dotted curve) and two- plus three-body hyperon-nucleon force in the original parametrization (I) (blue dashed curve) are displayed. As expected, the presence of hyperons makes the EOS softer. In particular, $\rho_\Lambda^{\text{th}} = 0.24(1) \text{ fm}^{-3}$ if hyperons

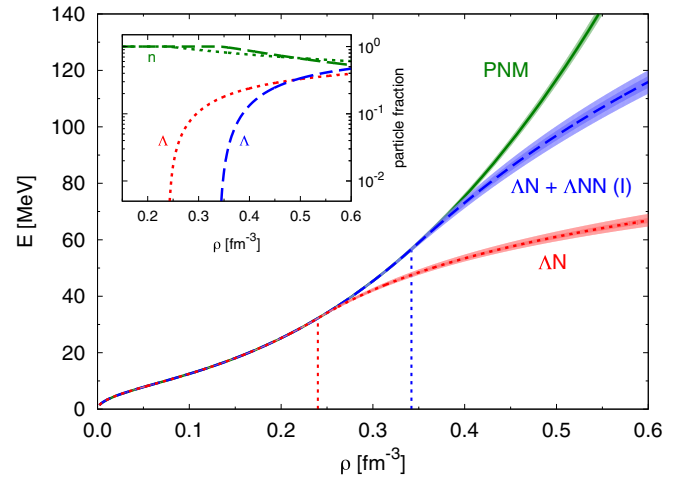


FIG. 1 (color online). Equations of state. Green solid curve refers to the PNM EOS calculated with the AV8' + UIX potential. The red dotted curve represents the EOS of hypermatter with hyperons interacting via the two-body ΛN force alone. The blue dashed curve is obtained including the three-body hyperon-nucleon potential in the parametrization (I). Shaded regions represent the uncertainties on the results as reported in the text. The vertical dotted lines indicate the Λ threshold densities ρ_Λ^{th} . In the inset, neutron and lambda fractions corresponding to the two HNM EOSs.

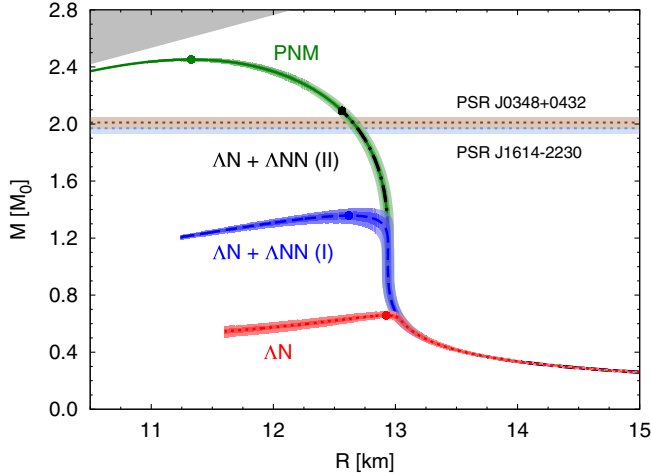


FIG. 2 (color online). Mass-radius relations. The key is the same as of Fig. 1. Full dots represent the predicted maximum masses. Horizontal bands at $\sim 2M_{\odot}$ are the observed masses of the heavy pulsars PSR J1614-2230 [18] and PSR J0348 + 0432 [19]. The grey shaded region is the excluded part of the plot due to causality.

only interact via the two-body ΛN potential. As a matter of fact, within the AFDMC framework hypernuclei turn out to be strongly overbound when only the ΛN interaction is employed [34,35]. The inclusion of the repulsive three-body force [model (I)], stiffens the EOS and pushes the threshold density to $0.34(1) \text{ fm}^{-3}$. In the inset of Fig. 1 the neutron and lambda fractions are shown for the two HNM EOSs.

Remarkably, we find that using the model (II) for ΛNN the appearance of Λ particles in neutron matter is energetically unfavored at least up to $\rho = 0.56 \text{ fm}^{-3}$, the largest density for which Monte Carlo calculations have been performed. In this case the additional repulsion provided by the model (II) pushes $\rho_{\Lambda}^{\text{th}}$ towards a density region where the contribution coming from the hyperon-nucleon potential cannot be compensated by the gain in kinetic energy. It has to be stressed that (I) and (II) give qualitatively similar results for hypernuclei. This clearly shows that an EOS constrained on the available binding energies of light hypernuclei is not sufficient to draw any definite conclusion about the composition of the neutron star core.

The mass-radius relations for PNM and HNM obtained by solving the Tolman-Oppenheimer-Volkoff equations [62] with the EOSs of Fig. 1 are shown in Fig. 2. The

onset of Λ particles in neutron matter sizably reduces the predicted maximum mass with respect to the PNM case. The attractive feature of the two-body ΛN interaction leads to the very low maximum mass of $0.66(2)M_{\odot}$, while the repulsive ΛNN potential increases the predicted maximum mass to $1.36(5)M_{\odot}$. The latter result is compatible with Hartree-Fock and Brueckner-Hartree-Fock calculations (see for instance Refs. [2–5]).

The repulsion introduced by the three-body force plays a crucial role, substantially increasing the value of the Λ threshold density. In particular, when model (II) for the ΛNN force is used, the energy balance never favors the onset of hyperons within the density domain that has been studied in the present work ($\rho \leq 0.56 \text{ fm}^{-3}$). It is interesting to observe that the mass-radius relation for PNM up to $\rho = 3.5\rho_0$ already predicts a NS mass of $2.09(1)M_{\odot}$ (black dot-dashed curve in Fig. 2). Even if Λ particles appear at higher baryon densities, the predicted maximum mass will be consistent with present astrophysical observations.

In this Letter we have reported on the first quantum Monte Carlo calculations for hyperneutron matter, including neutrons and Λ particles. As already verified in hypernuclei, we found that the three-body hyperon-nucleon interaction dramatically affects the onset of hyperons in neutron matter. When using a three-body ΛNN force that overbinds hypernuclei, hyperons appear at around twice the saturation density and the predicted maximum mass is $1.36(5)M_{\odot}$. By employing a hyperon-nucleon-nucleon interaction that better reproduces the experimental separation energies of medium-light hypernuclei, the presence of hyperons is disfavored in the neutron bulk at least up to $\rho = 0.56 \text{ fm}^{-3}$ and the lower limit for the predicted maximum mass is $2.09(1)M_{\odot}$. Therefore, within the ΛN model that we have considered, the presence of hyperons in the core of the neutron stars cannot be satisfactorily established and thus there is no clear incompatibility with astrophysical observations when lambdas are included. We conclude that in order to discuss the role of hyperons—at least lambdas—in neutron stars, the ΛNN interaction cannot be completely determined by fitting the available experimental energies in Λ hypernuclei. In other words, the Λ -neutron-neutron component of the ΛNN force will need both additional theoretical investigation, possibly within different frameworks such as chiral perturbation theory [63,64], and a substantial additional amount of experimental data, in particular for highly asymmetric hypernuclei and excited states of the hyperon.

We would like to thank J. Carlson, S.C. Pieper, S. Reddy, A.W. Steiner, W. Weise, and R.B. Wiringa for stimulating discussions. The work of D.L. and S.G. was supported by the U.S. Department of Energy, Office of Science, Office of Nuclear Physics, under the NUCLEI SciDAC grant and A.L. by the Department of Energy, Office of Science, Office of Nuclear Physics, under Contract No. DE-AC02-06CH11357. The work of S.G.

TABLE II. Fitting parameters for the function f defined in Eq. (4) for different hyperon-nucleon potentials.

Hyperon-nucleon potential	c_1 [MeV]	c_2 [MeV]
ΛN	$-71.0(5)$	$3.7(3)$
$\Lambda N + \Lambda NN$ (I)	$-77(2)$	$31.3(8)$
$\Lambda N + \Lambda NN$ (II)	$-70(2)$	$45.3(8)$

was also supported by DOE under Contract No. DE-AC02-05CH11231, and by a Los Alamos LDRD grant. This research used resources of the National Energy Research Scientific Computing Center (NERSC), which is supported by the Office of Science of the U.S. Department of Energy under Contract No. DE-AC02-05CH11231.

-
- [1] V. A. Ambartsumyan and G. S. Saakyan, *Sov. Astron. AJ* **4**, 187 (1960).
- [2] E. Massot, J. Margueron, and G. Chanfray, *Europhys. Lett.* **97**, 39002 (2012).
- [3] H. Đapo, B.-J. Schaefer, and J. Wambach, *Phys. Rev. C* **81**, 035803 (2010).
- [4] H.-J. Schulze and T. Rijken, *Phys. Rev. C* **84**, 035801 (2011).
- [5] I. Vidaña, D. Logoteta, C. Providência, A. Polls, and I. Bombaci, *Europhys. Lett.* **94**, 11002 (2011).
- [6] J. N. Hu, A. Li, H. Toki, and W. Zuo, *Phys. Rev. C* **89**, 025802 (2014).
- [7] T. Miyatsu, M.-K. Cheoun, and K. Saito, *Phys. Rev. C* **88**, 015802 (2013).
- [8] T. Miyatsu, S. Yamamuro, and K. Nakazato, *Astrophys. J.* **777**, 4 (2013).
- [9] N. Gupta and P. Arumugam, *Phys. Rev. C* **88**, 015803 (2013).
- [10] R. Mallick, *Phys. Rev. C* **87**, 025804 (2013).
- [11] I. Bednarek, P. Haensel, J. L. Zdunik, M. Bejger, and R. Mańka, *Astron. Astrophys.* **543**, A157 (2012).
- [12] S. Weissenborn, D. Chatterjee, and J. Schaffner-Bielich, *Phys. Rev. C* **85**, 065802 (2012).
- [13] W.-Z. Jiang, B.-A. Li, and L.-W. Chen, *Astrophys. J.* **756**, 56 (2012).
- [14] A. Sulaksono and B. Agrawal, *Nucl. Phys.* **A895**, 44 (2012).
- [15] L. L. Lopes and D. P. Menezes, *Phys. Rev. C* **89**, 025805 (2014).
- [16] S. E. Thorsett and D. Chakrabarty, *Astrophys. J.* **512**, 288 (1999).
- [17] D. J. Champion *et al.*, *Science* **320**, 1309 (2008).
- [18] P. B. Demorest, T. Pennucci, S. M. Ransom, M. S. E. Roberts, and J. W. T. Hessels, *Nature (London)* **467**, 1081 (2010).
- [19] J. Antoniadis *et al.*, *Science* **340**, 1233232 (2013).
- [20] A. W. Steiner and S. Gandolfi, *Phys. Rev. Lett.* **108**, 081102 (2012).
- [21] J. M. Lattimer and A. W. Steiner, *Astrophys. J.* **784**, 123 (2014).
- [22] A. T. Deibel, A. W. Steiner, and E. F. Brown, *Phys. Rev. C* **90**, 025802 (2014).
- [23] A. W. Steiner, J. M. Lattimer, and E. F. Brown, *Astrophys. J.* **722**, 33 (2010).
- [24] E. N. E. van Dalen, G. Colucci, and A. Sedrakian, *Phys. Lett. B* **734**, 383 (2014).
- [25] H.-J. Schulze, *J. Phys. Conf. Ser.* **336**, 012022 (2011).
- [26] D. Logoteta, C. Providência, and I. Vidaña, *Phys. Rev. C* **88**, 055802 (2013).
- [27] J. L. Zdunik and P. Haensel, *Astron. Astrophys.* **551**, A61 (2013).
- [28] M. Orsaria, H. Rodrigues, F. Weber, and G. A. Contrera, *Phys. Rev. C* **89**, 015806 (2014).
- [29] P. Char and S. Banik, *Phys. Rev. C* **90**, 015801 (2014).
- [30] S. Nishizaki, Y. Yamamoto, and T. Takatsuka, *Prog. Theor. Phys.* **105**, 607 (2001).
- [31] S. Nishizaki, Y. Yamamoto, and T. Takatsuka, *Prog. Theor. Phys.* **108**, 703 (2002).
- [32] Y. Yamamoto, T. Furumoto, N. Yasutake, and T. A. Rijken, *Phys. Rev. C* **88**, 022801 (2013).
- [33] Y. Yamamoto, T. Furumoto, N. Yasutake, and T. A. Rijken, *Phys. Rev. C* **90**, 045805 (2014).
- [34] D. Lonardoni, F. Pederiva, and S. Gandolfi, *Phys. Rev. C* **89**, 014314 (2014).
- [35] D. Lonardoni, S. Gandolfi, and F. Pederiva, *Phys. Rev. C* **87**, 041303 (2013).
- [36] B. S. Pudliner, V. R. Pandharipande, J. Carlson, S. C. Pieper, and R. B. Wiringa, *Phys. Rev. C* **56**, 1720 (1997).
- [37] R. B. Wiringa, V. G. J. Stoks, and R. Schiavilla, *Phys. Rev. C* **51**, 38 (1995).
- [38] R. B. Wiringa and S. C. Pieper, *Phys. Rev. Lett.* **89**, 182501 (2002).
- [39] S. C. Pieper, V. R. Pandharipande, R. B. Wiringa, and J. Carlson, *Phys. Rev. C* **64**, 014001 (2001).
- [40] S. Gandolfi, J. Carlson, and S. C. Pieper, *Phys. Rev. Lett.* **106**, 012501 (2011).
- [41] B. S. Pudliner, V. R. Pandharipande, J. Carlson, and R. B. Wiringa, *Phys. Rev. Lett.* **74**, 4396 (1995).
- [42] S. Gandolfi, J. Carlson, S. Reddy, A. W. Steiner, and R. B. Wiringa, *Eur. Phys. J. A* **50**, 10 (2014).
- [43] S. Gandolfi, J. Carlson, and S. Reddy, *Phys. Rev. C* **85**, 032801 (2012).
- [44] A. R. Bodmer, Q. N. Usmani, and J. Carlson, *Phys. Rev. C* **29**, 684 (1984).
- [45] M. Imran, A. A. Usmani, M. Ikram, Z. Hasan, and F. C. Khanna, *J. Phys. G* **41**, 065101 (2014).
- [46] A. A. Usmani and F. C. Khanna, *J. Phys. G* **35**, 025105 (2008).
- [47] Q. N. Usmani and A. R. Bodmer, *Phys. Rev. C* **60**, 055215 (1999).
- [48] A. A. Usmani, S. C. Pieper, and Q. N. Usmani, *Phys. Rev. C* **51**, 2347 (1995).
- [49] A. A. Usmani, *Phys. Rev. C* **52**, 1773 (1995).
- [50] A. R. Bodmer and Q. N. Usmani, *Nucl. Phys.* **A477**, 621 (1988).
- [51] A. R. Bodmer and Q. N. Usmani, *Phys. Rev. C* **31**, 1400 (1985).
- [52] E. Hiyama, M. Kamimura, Y. Yamamoto, and T. Motoba, *Phys. Rev. Lett.* **104**, 212502 (2010).
- [53] A. Gal and D. J. Millener, *Phys. Lett. B* **701**, 342 (2011).
- [54] J. Schaffner, C. B. Dover, A. Gal, C. Greiner, and H. Stöcker, *Phys. Rev. Lett.* **71**, 1328 (1993).
- [55] J. Schaffner, C. B. Dover, A. Gal, C. Greiner, D. J. Millener, and H. Stöcker, *Ann. Phys. (N.Y.)* **235**, 35 (1994).
- [56] J. Schaffner-Bielich and A. Gal, *Phys. Rev. C* **62**, 034311 (2000).
- [57] K. E. Schmidt and S. Fantoni, *Phys. Lett. B* **446**, 99 (1999).
- [58] S. Gandolfi, A. Y. Illarionov, S. Fantoni, J. C. Miller, F. Pederiva, and K. E. Schmidt, *Mon. Not. R. Astron. Soc.* **404**, L35 (2010).
- [59] S. Gandolfi, A. Y. Illarionov, K. E. Schmidt, F. Pederiva, and S. Fantoni, *Phys. Rev. C* **79**, 054005 (2009).
- [60] A. Sarsa, S. Fantoni, K. E. Schmidt, and F. Pederiva, *Phys. Rev. C* **68**, 024308 (2003).
- [61] S. Gandolfi, A. Lovato, J. Carlson, and K. E. Schmidt, *Phys. Rev. C* **90**, 061306 (2014).
- [62] J. R. Oppenheimer and G. M. Volkoff, *Phys. Rev.* **55**, 374 (1939).
- [63] J. Haidenbauer, S. Petschauer, N. Kaiser, U.-G. Meißner, A. Nogga, and W. Weise, *Nucl. Phys.* **A915**, 24 (2013).
- [64] N. Kaiser and W. Weise, *Phys. Rev. C* **71**, 015203 (2005).